Journal of Chromatography A, 1218 (2011) 997–1003

Contents lists available at ScienceDirect

Journal of Chromatography A

journal homepage: www.elsevier.com/locate/chroma

# On-chip fraction collection for multiple selected ssDNA fragments using isolated extraction channels

Zheyu Li [a], Kai Sun [a,**], Misato Sunayama [b], Yasutaka Matsuo [a], Vygantas Mizeikis [c], Ryoko Araki [b], Kosei Ueno [a], Masumi Abe [b], Hiroaki Misawa [a,*]

[a] Research Institute for Electronic Science, Hokkaido University, Kita-21 Nishi-10, Kita-ku, Sapporo 001-0021, Hokkaido, Japan
[b] National Institute of Radiological Sciences, Chiba, Japan
[c] Division of Global Research Leaders and Research Institute of Electronics, Shizuoka University, Hamamatsu, Japan

ARTICLE INFO

*Article history:*
Received 8 October 2010
Received in revised form
16 December 2010
Accepted 19 December 2010
Available online 28 December 2010

*Keywords:*
Multi-target
Fraction collection
Fractionation
Electrophoresis
Contamination
Isolated extraction channels

ABSTRACT

High efficiency and high-purity fraction collection is highly sought in analysis of fragments-of-interest from selective polymerase chain reaction (PCR) products generated by High Coverage Gene Expression Profiling (HiCEP) methods. Here we demonstrate a new electrophoretic chip device enabling automatic high-efficient fractionation of multiple ssDNA target fragments during a run of separation. We used thoroughly isolated extraction channels for each selected target to reduce the risk of cross-contamination between targets due to cross-talk of extraction channels. Fragments of 35, 108 and 138 b, were successfully isolated, then the recovery was PCR-amplified and assessed by capillary electrophoresis (CE) analysis. Total impurity level of the targets due to unwanted fragments of 0.7%, 2% and 6% respectively, was estimated. Difficulties in collecting multiple target factions are due to band diffusion and DNA adsorption to the walls for the fragments in the separation channel, which is generated by transferring the DNA target fraction from the extraction section to the target reservoir. Therefore, we have carefully measured band broadening and analyzed its influence on the separation resolution due to the delay.



## 1. Introduction

Transcriptome studies of gene expression and regulation mechanisms are among the most important areas of post-genome research [1–6]. Gene expression analysis is usually performed using DNA microarrays. This technique uses an array of oligo-nucleotides derived from cDNA synthesized from mRNA templates, and can only be used to profile known genes. In general, sensitivity of this technique is low, and differences in mRNA expression less than a factor of two or three cannot be detected. To overcome these difficulties, a method based on cDNA-Amplified Restriction Fragment Length Polymorphism (AFLP), called High Coverage Gene Expression Profiling (HiCEP) has been developed [7]. Because HiCEP data is based on cDNA fragments obtained using restriction enzymes, it can be used to profile unknown transcripts as well as known genes. However, like all the AFLP methods, it requires isolation of fragments-of-interest from selective polymerase chain reaction (PCR) products in order to accomplish the sequencing. The conventional fraction collection technique based on slab gel electrophoresis is time-consuming with their typical requirement of overnight pre-run time, and has insufficient resolution of the separation. Moreover, its reproducibility is poor due to the subjectiveness of human operator, and inaccuracy of the pickup tools used, whose selectivity exceeds the band spacing.

Liquid chromatography technology provides the means for separation and fraction collection of organic molecules and DNA, or peptides and proteins. Lim et al. has collected eluted fractions during denaturing high-performance liquid chromatography analysis of mitochondrial DNA mutation [8]. Capillary electrophoresis (CE) has become widely used in molecular diagnostic laboratories, mainly because of its single base resolution and ability to automate both loading and analysis. CE is not only an analytical technique but it can also be used for collection [9–12]. Lin et al. designed and constructed an alternative block for the ABI 310 CE instrument, capillary electrophoresis was stopped before the desired molecules migrating to the end of the capillary, and original standard gel block was then replaced by a reconfigured gel block holding a collection tube. The reconfigured system allows collection with a resolution of as high as three bases [13]. However, the collection resolution of both methods is limited by their 1D nature and absence of real-time detection capability. Microfluidic chips available due to advances in

* Corresponding author. Tel.: +81 11 706 9358; fax: +81 11 706 9359.
** Corresponding author. Tel.: +81 11 706 9340; fax: +81 11 706 9376.
*E-mail addresses:* ksun@es.hokudai.ac.jp (K. Sun), misawa@es.hokudai.ac.jp (H. Misawa).

0021-9673/$ – see front matter © 2010 Elsevier B.V. All rights reserved.
doi:10.1016/j.chroma.2010.12.089

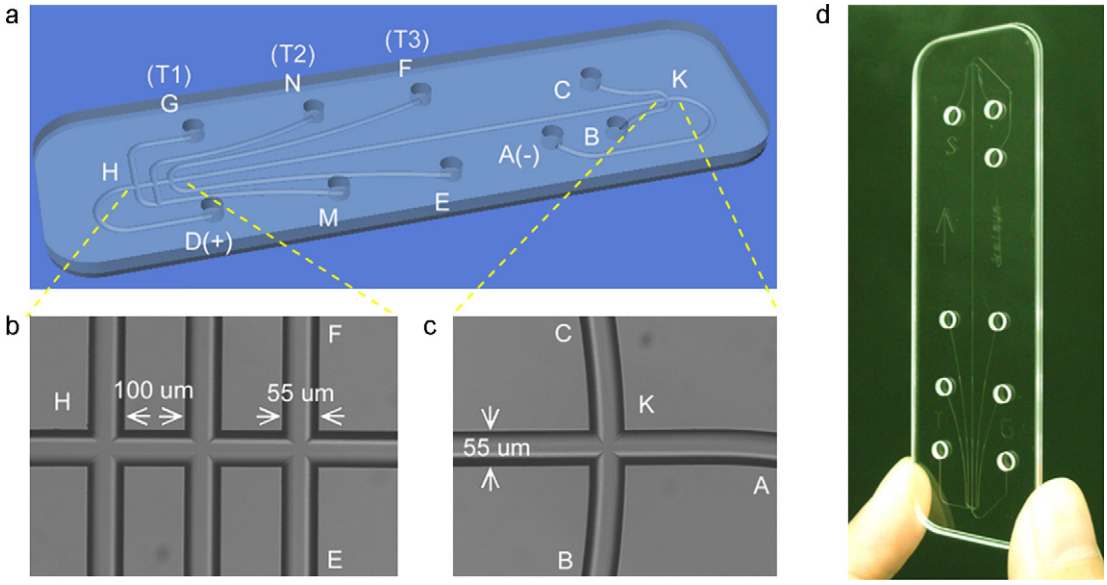


**Fig. 1.** 3D schematic drawing of the microfabricated device with the microfluidic channels (a), 87 mm effectively long straight separation channel (K–H), focusing channel (E–H/F–H), and extraction channel (M–G, M–N and E–F). 9 reservoirs of the buffer (A), sample waste (B), sample (C), buffer waste (D), focusing (E and F), and target (G, N and F) are marked. Microscopic images of the intersections of extraction (b) and injection (c), and photograph of the microchip (d). The interval distance between the parallel extraction channels is 100 μm. All the channels are 55 μm wide and 25 μm deep.

2D fabrication methods [14–23] have enabled replacement of the capillaries by more modern techniques of separation and fraction collection. Two novel on-chip structures for continuous-flow fraction collection [17,18] have been proposed to obtain much more recovery. However, it is difficult to apply to high-resolution DNA fraction collection. Earlier, we have shown high-resolution and high-fidelity fraction collection of ssDNA fragments differing in size by one base on a spiral-channel glass chip [20]. The combination of a long spiral channel with a small microchannel cross-section, a short injection plug, and automated fragment selection and extraction algorithm was instrumental in achieving the record-high resolution at low impurity levels. In addition to improving the resolution and reducing the cross-contamination, high throughput is also essential in the collection of multiple target fragments for lower sample and reagent consumption, shorter running time and lower running costs. We have shown a method for multiple fraction collection during a run of separation, in which four transfer sub-channels are connected to an extraction channel [23]. In this case, all targets have to share the same extraction channel, which increases the risk of cross-contamination.

Here, we present high-efficiency and high-fidelity fraction collection with a novel three-parallel isolated extraction-channel structure on a 3 cm × 10 cm × 0.2 cm quartz chip. The isolated extraction channel for each target may reduce cross contamination between collections due to sharing one extraction/transferring channel. We monitored fluorescence flux at the extraction intersections and optimized conditions for collection procedures, and with which we achieved collection of three selected targets with low ratio of impurities during one run of separation. Difficulties in collecting of multiple target factions are due to delay time necessary for transferring the DNA target fraction from the extraction section to the target reservoir. The delay may result in band broadening of the fragments in the main separation channel, degrading the resolution and even overlapping the neighboring bands. As a result, subsequent collections may become difficult. Therefore, we have carefully measured band broadening and analyzed its influence on the resolution of separation due to the delay time.

## 2. Materials and methods

POP-4 matrix, 10× running buffer, Hi-deionized formamide solution, GeneScan 500 ROX, and BigDye Terminator v3.1 Cycle Sequencing Kit for separation in capillaries and microchannels from PE Applied Biosystems (USA) were used. All other required chemicals were supplied by Wako Pure Chemical Industries (Japan). Water was purified by reverse osmosis followed by treatment by Milli-Q Plus ion exchange and organic adsorption cartridges (Millipore). HiCEP method and determination of impurities in the recovery by PCR and CE analysis were the same as described in our previous work [7].

### 2.1. Chip design and fabrication

The chips were fabricated using standard photolithography and wet-etching techniques [20]. Photomask for pattern transfer was designed using AutoCAD (AutoDesk, Inc., USA) and subsequently fabricated by Micro Electronic Technology Development Application Corp., (Beijing, China). The microfluidic structure (Fig. 1) fabricated on a 30 mm × 100 mm × 0.5 mm quartz wafer, consist of nine 3-mm-diameter reservoirs, a typical injector unit, a 87-mm-long straight separation channel, and three parallel channels for the extraction and retrieval of the target. The channels were 55 μm-wide and 25 μm-deep. The interval between parallel channels was 100 μm. Access holes serving as reservoirs were drilled into the 1.5-mm-thick cover plate with diamond-tipped drill. The channel plate and the cover plate were thermally bonded at the glass transition temperature of $T_g$ = 1070 °C for 3 h.

### 2.2. Electrophoretic separation

First, POP-4 matrix was injected into the channels. An aliquot of 2.0 μl of the PCR products labeled with three different fluorescent dyes or 0.2 μl of GeneScan 500 ROX (Applied Biosystems), and 15 μl of formamide was then mixed, denatured by incubation at 95.0 °C for 2 min and chilled on ice for 5 min. The mixed solution was loaded on the chip. The sample was loaded from C

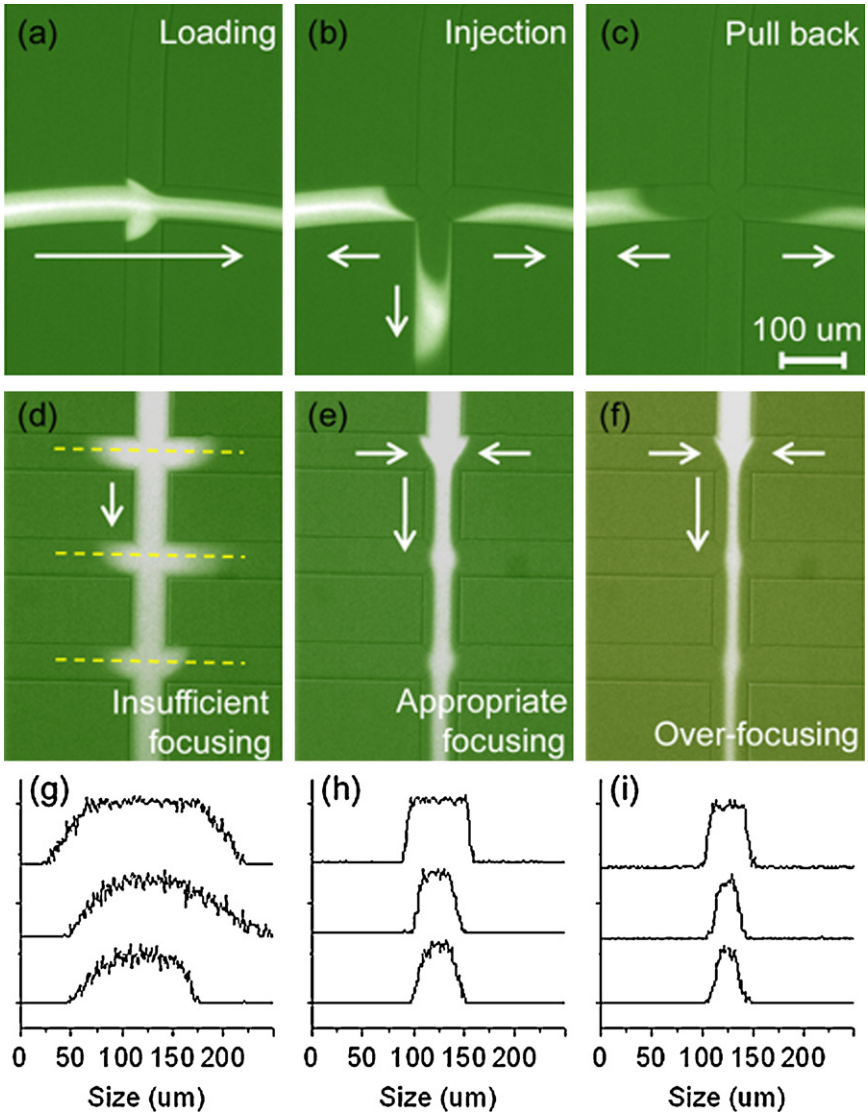


**Fig. 2.** Fluorescence images of the procedures: sample loading (a), sample injection into the separation channel (b), pull-back to cut off the leakage (c) at the injection intersection. Comparison of insufficient-focusing (d), appropriate focusing (e) and over-focusing (f) by applying a different bias potential 2000 V, 1500 V and 1200 V on the reservoir of E and F. The line-profile analysis on each extraction intersection is shown under the fluorescence images (g–i).

to B at 200 V/cm for 100 s (Fig. 2(a)), and then injected into the separation channel for 1 s (Fig. 2(b)). Injection and separations for ssDNA fragments were performed at 200 V/cm, with the injection plug approx. 150 μm long (Fig. 2(b)). The samples were then driven to the anode (reservoir D, Fig. 1(a)). The above described separation and fractionation procedures were performed at room temperature.

An inverted microscope (IX71, Olympus, Japan) with a fluorescence filter unit (Dichronic mirror: 505 nm; Emission: 510 nm~IF) and a 12-bit digital CCD camera (Hamamatsu: ORCA-EG, Japan) were used for fluorescence imaging. A mercury lamp was used as the source of fluorescence excitation in order to monitor and optimize collection conditions (Figs. 2 and 3). A 488-nm argon ion laser illumination (177G-UK01, Spectra Physics Laser, USA) with 50 mW output power was used to improve S/N ratio of segment recognition in the application of resolution measurement and multiple collections. The rest of experimental setup was the same as described in our previous works [20,23].

### 2.3. Monitoring of the band broadening

The fluorescently labeled ssDNA ladder (GeneScan 500 ROX, 35–500 bases) was separated in a length of 87 mm (K–H), and was stopped close to the detector (H) by turning off the electric field. Then the DNA fragments were allowed to diffuse in the POP-4 matrix in absence of the electric field. After a delay, the separation was restarted and the peak was detected during passage through the detector [24]. Full width at half-height of the obtained peaks was then compared with the separation in absence of delay.

## 3. Results and discussion

Fraction collection of multiple selected ssDNA fragments successively with only one run of electrophoretic separation may become a way for high-throughput fraction collection, which is often desired during HiCEP analysis. However, sharing of the extraction channel results in cross-contamination easily. Further-

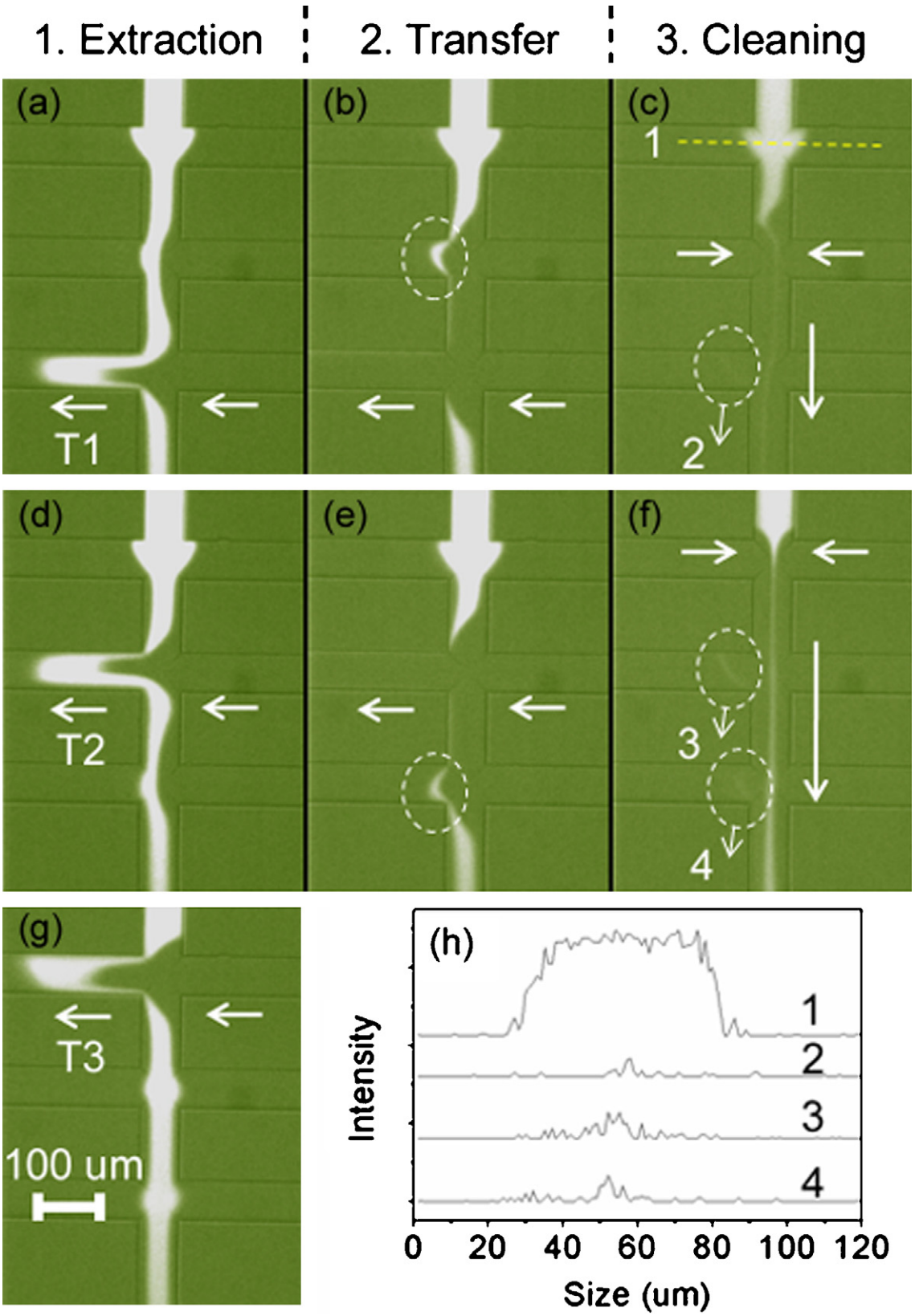


**Fig. 3.** The operating flow of the collection procedure: extraction, transfer and cleaning of three-target collections in succession. Four line-profile analysis for the marked area in (c) and (f) is shown in (h).

more, bands of the fragments in the separation channel may diffuse during the delay time between two collections. This will affect resolution of the separation negatively. These issues will be discussed below.

### 3.1. Procedures of multiple target collections

For high-efficiency fraction collection, we have developed a structure containing three parallel channels instead of single extraction channel. Each channel corresponds to one extraction, and the extraction channel order for Targets 1–3 is from left to right (Fig. 1(b)). Figs. 2 and 3 show the separation and collection procedure at the injection intersection K and the extraction intersections H. Here, fluorescence flux of SYBR Green II stained 100-base fragment (Invitrogen Life Technologies, Japan) was used in order to monitor any sensitive variance during the collection. In this study, in order to suppress the contamination, same potential is applied to the reservoir E and F to block unselected fragments entering into extraction channels (hereafter called focusing, the focusing method was introduced to decrease the volume of injection plug on microfluidic devices [25]). As shown in Fig. 2(e), the bands therefore become narrowed by focusing; they then pass through the three intersections retaining their narrow shape. Separation without focusing or with insufficient focusing (Fig. 2(d)) may result in a problem, namely, contamination due to unwanted passing fragments which may enter the extraction channels. Line profile analysis (Fig. 2(g)–(i)) shows the fluorescence-intensity distribution at the three intersections, illustrating that there is no leakage into the extraction channel. It should be noted that too low focusing potential (hereafter called over-focusing, Fig. 2(f)) decreases electric field in the separation channel, which leads to separation velocity lower by about 20%. Moreover, over-focusing also results in low recovery volume.

For each target extraction, all separation electrodes were isolated from the electric field, while bias was applied to corresponding extraction channels (Fig. 3(a), (d)and (g)). Finally, transfer operation was carried out for 60 s in order to drive the extracted target to the target reservoir G/N/F respectively. During the transfer of Target 1, we found a band distortion occurring near the middle intersection (Fig. 3(b)) due to halt of the focusing, and partial sharing of channels M–G and M–N. If not moved out of the middle extraction channel, this band will absolutely contaminate subsequent Target 2. Hence, a cleaning procedure as shown in Fig. 3(c) is essential to guarantee non-contamination in the channel before the next target extraction. The cleaning involves similar manipulations as the focusing, with the only difference that the corresponding electrodes are grounded during the cleaning. Although a very small band generated by cleaning can be detected at the entrance of the down-most extraction channel for Target 1 (Fig. 3(c and h)), Target 1 is already transferred into the target reservoir G, and therefore cannot be contaminated. The transfer of Target 2 also generates a band distortion on the first extraction channel (Fig. 3(e)), but it can be ignored due to the same reason as described above. Before the extraction of Target 3, a cleaning (Fig. 3(f)) is used to remove the contamination from two sides of the arrow at the up-most extraction intersection. The procedure thus enables on-chip multiple fraction collection in succession with one run of separation.

### 3.2. Application of three-target collections for HiCEP analysis

Fragments of 35, 108 and 138-base long in HiCEP products of mouse embryonic stem (ES) cell E14 (E14-inc-H(−)-1-1-P1_B01) were selected for collection with one separation run on the chip. Before fractionation a run of electrophoretic separation was carried out in order to detect features such as position and peak width

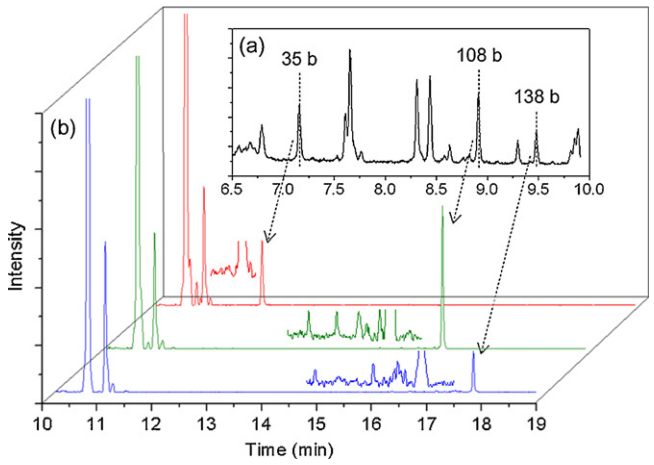


**Fig. 4.** Electrophoretograms of the HiCEP analysis product (E14-inc-H(−)-1-1-P1_B01) separated on a 8.7 cm long channel chip (a) and CE analysis of the on-chip fractionated samples (35 b, 108 b and 138 b) on a PRISM3100 genetic analyzer with a 47 cm long (36 cm to the detector) fused silica capillary (b).

of the selected targets. The electrophoretogram of the E14-inc-H(−)-1-1-P1_B01 separated on the chip is shown in Fig. 4(a). The three dashed lines on the target peaks in Fig. 4(a) show the positions of collection where they are close to the center of each peak. Using the above procedures, the targets were extracted and transferred into the target reservoirs G, N and F in succession. Below, we discuss the evaluation of the discovery. Any peak purity determination can only confirm the presence of impurities and never prove absolutely that the peak is pure. The likelihood of discovering an impurity increases with the resolution between target and impurity, as well as with absolute and relative concentration of the sample. Therefore, we initially amplified the recovery by 28 cycles of PCR to increase the concentration, and then performed CE analysis using PRISM3100 genetic analyzer with a 47 cm long (36 cm at the detector) fused silica capillary. The electrophoretograms are shown in Fig. 4(b).

All the baselines in Fig. 4(b) are very flat, and no obvious contamination in any of the three electrophoretograms was observed. In order to assess the existence of small contamination, all the peak profiles were magnified and analyzed. The ratio of peak area of the unselected peaks to the target peak ($I_u/I_t$) according to the CE analysis was used to evaluate the contamination. The leftmost peaks in all checks, which come from primer dimer and primers during PCR, were not considered in the contamination calculation. Thorough analysis has revealed that purity of the recovery of 35 b was very satisfactory, the contamination rate was only about 0.7% which was even close to the standard deviation of the baseline. According to the magnified peak profiles (Fig. 4(b)), some very small peaks before the targets were identified in the recovery of 108 b and 138 b. Furthermore, these contamination peaks were in a certain range before the targets, and there was no contamination from much smaller size DNA fragment than the targets. The contamination rates of the recovery of 108 b and 138 b were 2.1% and 6.3% respectively. By comparison of the total peak area of the unselected peaks in the recovery of 108 b and 138 b, we found that the absolute area of them is roughly similar. However, the contamination evaluation in our work is a relative value to the target peak area. One can see that the target peak of 138 b was smaller than 108 b (Fig. 4(a)), therefore the contamination rate of the recovery of 138 b fragment was higher than that of 108 b fragment.

Although impurity of the recovery was very low, and did not degrade the quality for the subsequent biotesting, it is relevant to discuss the possible sources of contamination. It may also explain

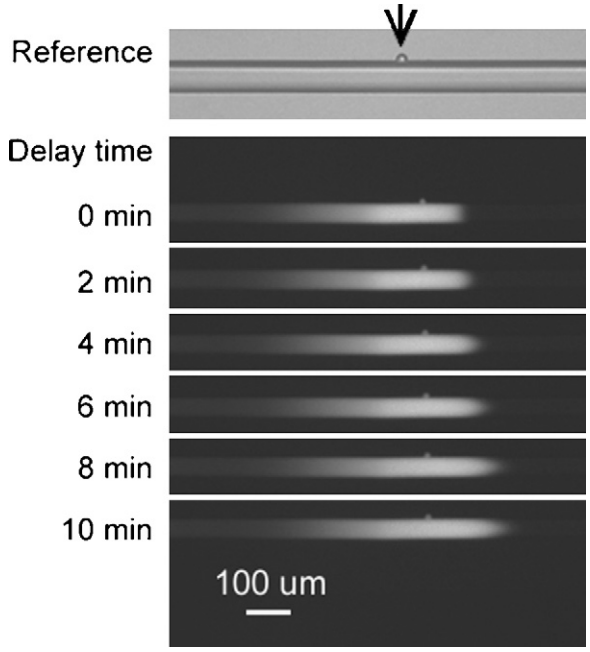


**Fig. 5.** Fluorescence images of 100 base fragment diffusing in POP-4 polymer over time in a microchip. A mercury lamp and SYBT Green II were utilized. 2 μl of 10 bp dsDNA ladder (Invitrogen Life Technologies, Japan) in 14 μl of formamide was denatured at 95 °C for 2 min and chilled on ice for 5 min. Then the sample was stained by SYBR Green II (1000:1) for 15 min. The fragment migrated to anode (from left to right in the images) before the electric field was turned off. According to a reference defect in the channel, the band broadening and the band-shape changing can be clearly confirmed.

why the absolute impurities to 108 b and 138 b are higher than that to 35 b.

### 3.3. Influence of the delay during multiple collections

Halting the migration of fragments in the separation channel for the target extraction and transferring the target to the destination generated a delay which definitely led to band diffusion of these fragments [26,27]. Fig. 5 shows series of fluorescence images of SYBR Green II stained 100-b fragment (Invitrogen Life Technologies, Japan) over a delay time from 0 to 10 min by turning off the electric field. One can see that the band width became wider and wider over time due to band diffusion. In the first image (no delay), the band was observed to have a flat front due to DNA molecules moving evenly toward the anode under very low EOF condition (the electroosmotic mobility $\mu_{eof}$: $\sim 10^{-5}$ cm$^2$ V$^{-1}$ s$^{-1}$). It is well-known that DNA adsorption leads to reduced signal levels, strongly asymmetric peaks, and surface charge on the wall. From the sequent images the flat front became parabolic after turning off the electric field, and the parabolic front became obvious as delay time increased. This phenomenon may be explained by that DNA molecules adsorbed at the channel walls and then it led to slow diffusion along the wall. The peak tailing in Fig. 5 may confirm the existence of DNA adsorption during delay time. Furthermore, the adsorbed molecules may be pulled and exfoliated by electrophoretic force and/or scratched off the wall by migrating DNA molecules in the continuous separation over time. This may explain why impurities are more likely to originate from the neighboring peaks.

Below, we would like to discuss influence of the delay on separation resolution during multiple collections. Band broadening due to the delay will degrade the identification resolution of the separation system and even overlap the neighboring peaks. As a result, subsequent collections may become difficult. Separation resolution per base ($R_b$) as obtained by Eq. (1), is defined by separation between two peaks, $\Delta X$, and the average peak width, $W$ as follows:

$$R_b = \frac{\Delta X}{N(W_{h1} + W_{h2})} \quad (1)$$

where $W_h$ is the peak width measured at half height, and $N$ is the base number difference between the two neighboring peaks [28]. In a measurement of the diffusion coefficient, same fragment was allowed to diffuse over different delay time. However, multiple-target collections involve same transfer time after each collection. This means that delay time for the final target is therefore much longer than that for the first peak.

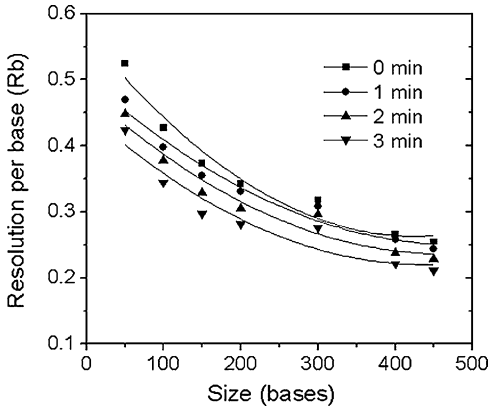


**Fig. 6.** The resolution per base of GeneScan-500 ROX ssDNA markers separated on the chip with the delay time of 0, 1, 2, and 3 min before each band passed through the detector.

A total of seven peaks from 50 b to 450 b were delayed one by one before passing through the detector, and delay time between two fragments was 0, 1, 2, and 3 min. The first peak of 50 b was also delayed in the measurement. Thus, the final peak of 450 b was delayed for 7, 14 and 21 min. The delay time was taken into account when calculating peak spacing. The achieved resolution, calculated by Eq. (1) is shown in Fig. 6. In order to collect a sample without contamination by electrophoresis, the target peak desires no overlap with neighbor peaks theoretically ($R_b \geq 1$ for one-base difference in size from neighbor fragment). Such resolution is twice higher than that required for sequencing ($R_b \geq 0.5$). Fig. 6 depicts the decrease of resolution with delay time. Comparing with the delay time of 0 min, the resolution of the fragments which are bigger than 200 b in case of 1 min delay decreases very little. For both the delay time of 0 and 1 min, our method can perform collection for 8 target fragments less than ~450 b with the resolution of more than a four-base difference in size from neighbor fragments ($R_b \geq 0.25$). When the delay time is up to 3 min, the available range of fragment size reduces to ~300 b in case of four-base difference in size from neighbor fragments. Hence, in a high-throughput application of fraction collection the available range may reduce significantly due to the delay, a higher separation resolution or faster transfer are therefore desired in the future work.

## 4. Concluding remarks

We have proposed a method which can realize on-chip successive collections of selected ssDNA fragments using isolated extraction channels. Using isolated extraction channels decrease the risk of cross-contamination from targets due to sharing the same extraction channel. Monitoring the fluorescence flux during focusing and extraction was helpful in finding ways to reduce or avoid the contamination. The successful application of this method is evidenced by very low impurity levels assessed via CE separation of the PCR-amplified recovery. Analysis on the influence of the delay on multiple collections

demonstrated that high-throughput may be possible by further improvement of transfer. The demonstrated high performance of fractionation-integrated electrophoretic microfluidic device may become a new powerful analytical tool for bioanalysis and related applications.

## Acknowledgments

The authors would like to gratefully acknowledge Mr. Tatsuji Meike for mechanical fabrication and assembly techniques. This work was supported by funding from the Japan Science and Technology Agency: Development of Systems and Technology for Advanced Measurement and Analysis Project, and from the Ministry of Education, Culture, Sports, Science, and Technology of Japan: KAKENHI Grant-in-Aid (no. 19049001) for Scientific Research on the Priority Area "Strong Photon-Molecule Coupling Fields for Chemical Reactions" (no. 470), and Grant-in-Aid from Hokkaido Innovation through Nanotechnology Support (HINTS).

## References

[1] S. Saha, A.B. Sparks, C. Rago, V. Akmaev, C.J. Wang, B. Vogelstein, K.W. Kinzler, V.E. Velculescu, Nat. Biotechnol. 20 (2002) 508.
[2] F.S. Collins, M. Morgan, A. Patrinos, Science 300 (2003) 286.
[3] S. Panda, M.P. Anotoch, B.H. Miller, A.I. Su, A.B. Schook, M. Straume, P.G. Schultz, S.A. Kay, J.S. Takahashi, J.B. Hogenesch, Cell 109 (2002) 307.
[4] D.J. Lockhart, H. Dong, M.C. Byrne, M.T. Follettie, M.V. Gallo, M.S. Chee, M. Mittmann, C. Wang, M. Kobayashi, H. Horton, et al., Nat. Biotechnol. 14 (1996) 1675.
[5] X. Wang, S. Ghosh, S.W. Guo, Nucleic Acids Res. 29 (2001) e75.
[6] D.D. Bowtell, Nat. Genet. 21 (1999) 25.
[7] R. Fukumura, H. Takahashi, T. Saito, Y. Tsutsumi, A. Fujimori, S. Sato, K. Tatsumi, R. Araki, M. Abe, Nucleic Acids Res. 31 (2003) e94.
[8] K.S. Lim, R.K. Naviaux, S. Wong, R.H. Haas, J. Mol. Diagn. 10 (2008) 102.
[9] M. Minarik, F. Foret, B.L. Karger, Electrophoresis 21 (2000) 247.
[10] P.O. Ekstrom, K. Khrapko, X. Li-Sucholeiki, L.W. Hunter, W.G. Thilly, Nat. Protocols 3 (2008) 1153.
[11] T. Irie, T. Oshida, H. Hasegawa, Y. Matsuoka, T. Li, Y. Oya, T. Tanaka, G. Tsujimoto, H. Kambara, Electrophoresis 21 (2000) 367.
[12] M. Minarik, K. Kleparnik, M. Gilar, F. Foret, A.W. Miller, Z. Sosic, B.L. Karger, Electrophoresis 23 (2002) 35.
[13] M. Lin, R.G. Rich, R.F. Shipley, M.J. Hafez, L. Tseng, K.M. Murphy, C.D. Gocke, J.R. Eshleman, J. Mol. Diagn. 9 (2007) 598.
[14] R. Sinville, A.S. Soper, J. Sep. Sci. 30 (2007) 1714.
[15] T. Footz, S. Wunsam, S. Kulak, H.J. Crabtree, D.M. Glerum, C.J. Backhouse, Electrophoresis 22 (2001) 3868.
[16] J. Khandurina, T. Chovan, A. Guttman, Anal. Chem. 74 (2002) 1737.
[17] L.R. Huang, J.R. Tegenfeldt, J.J. Kraeft, J.C. Sturm, R.H. Austin, E.C. Cox, Nat. Biotechnol. 20 (2002) 1048.
[18] C.A. Baker, M.G. Roper, J. Chromatogr. A 1217 (2010) 4743.
[19] J.J. Tulock, M.A. Shannon, P.W. Bohn, J.V. Sweedler, Anal. Chem. 76 (2004) 6419.
[20] K. Sun, N. Suzuki, Z.-Y. Li, R. Araki, K. Ueno, S. Juodkazis, M. Abe, S. Noji, H. Misawa, Electrophoresis 30 (2009) 4277.
[21] R.S. Lin, D.T. Burke, M.A. Burns, J. Chromatogr. A 1010 (2003) 255.
[22] R.S. Lin, D.T. Burke, M.A. Burns, Anal. Chem. 77 (2005) 4338.
[23] K. Sun, Z.-Y. Li, K. Ueno, S. Juodkazis, S. Noji, H. Misawa, Electrophoresis 28 (2007) 1572.
[24] A.E. Nkodo, J.M. Garnier, B. Tinland, H. Ren, C. Desruisseaux, L.C. McCormick, G. Drouin, G.W. Slater, Electrophoresis 22 (2001) 2424.
[25] L.M. Fu, R.J. Yang, G.B. Lee, Anal. Chem. 75 (2003) 1905.
[26] A.E. Nkodo, B. Tinland, Electrophoresis 23 (2002) 2755.
[27] J. Mercier, G.W. Slater, Electrophoresis 27 (2006) 1453.
[28] C. Heller, Electrophoresis 22 (2001) 629.